ELSEVIER

Biomaterials 19 (1998) 1101–1107

Biomaterials

Preparation of high-temperature stabilized β-tricalcium phosphate by heating deficient hydroxyapatite with $Na_4P_2O_7 \cdot 10H_2O$ addition

Feng-Huei Lin[a], Chun-Jen Liao[b], Ko-Shao Chen[b], Jui-Sheng Sun[c,*]

[a] *Center for Biomedical Engineering, College of Medicine, National Taiwan University, Taipei, Taiwan, ROC*
[b] *Department of Material Engineering, Tatung Technology Institute, Taipei, Taiwan, ROC*
[c] *Department of Orthopaedic Surgery, College of Medicine, National Taiwan University, Taipei, Taiwan, ROC*

Received 28 April 1997; accepted 25 January 1998

Abstract

In this paper, the high-temperature stabilized β-tricalcium phosphate (βTCP, β-$Ca_3(PO_4)_2$) were prepared by heating the deficient HAP (d-HAP, $Ca_{10-x}(HPO_4)_x(PO_4)_{6-x}(OH)_{2-x}$) with tetra-sodium diphosphate decahydrate (NP, $Na_4P_2O_7 \cdot 10H_2O$) addition. The βTCP, d-HAP and d-HAP doped with 2.5, 5, 7.5 and 10 wt % NP were heated to different temperatures and were investigated by X-ray diffraction analysis (XRD) and Fourier-transformed infrared spectroscopy (FTIR). The results demonstrated that the HPO_4^{2-} of d-HAP condensed into $P_2O_7^{4-}$ occurred before 650°C. The $P_2O_7^{4-}$ ions could be traced in the FTIR spectrum when the d-HAP was heated up to 750°C. The reaction of $P_2O_7^{4-}$ with OH^- did not occur instantly but over a wide range of temperatures. The d-HAP doped with NP would decrease the decomposition temperature of d-HAP. NP doped into d-HAP not only induced the d-HAP decomposition at lower temperature but also stabilized the βTCP crystal structure at higher-temperature. It could also increase the conversion temperature of βTCP to αTCP from 1180°C up to 1300°C. We could successfully prepare high-temperature (up to 1300°C) stabilized βTCP by heating NP doped d-HAP. © 1998 Published by Elsevier Science Ltd. All rights reserved

Keywords: Tricalcium phosphate; Bioresorbable; Phase transformation

1. Introduction

β-tricalcium phosphate (βTCP, β-$Ca_3(PO_4)_2$) is currently used as bone graft replacement material. It is well known that the βTCP have exceptionally good tissue compatibility, direct bonding to regenerated bone without intermediate connective tissue, faster bone regeneration, and resorbability as well [1–4]. However, βTCP ceramic is difficult to densify because high densification requires higher temperatures, but a sintering temperature beyond 1180°C induces the phase transformation of β to α-tricalcium phosphate (αTCP). The density of αTCP has a lower density than that of βTCP (αTCP: 2.77, βTCP: 3.07 $g\,cm^{-3}$). The volume of sintered TCP will expand and the crack will generate inside the material while the phase transformation of βTCP to αTCP occurrs. It would lead to a doubtful mechanical stability under the physiological loading [4]. Therefore, it is important to stabilize the crystalline phase of βTCP at higher temperatures.

The Mg ions have been chosen to dope the TCP material, which could replace the Ca ion position in the lattice of β-whitlockite to form compounds of $Mg_3(PO_4)_2$ or $Ca_{3-x}Mg_x(PO_4)_2$. These compounds could effectively stabilize the β-whitlockite structure at high temperatures [5–8]. However, the precursor of Mg ion, such as $MgCl_2$, $Mg(OH)_2$ or $MgCO_3$, would form other stable inclusions such as chlorined-HAP ($Ca_{10}(PO_4)_6(Cl)_2$) or remain difficult to remove magnesium oxide (MgO) in the TCP material during heat treatment. It would influence the mechanical strength of the TCP and the performance in the physiological environment. In addition, some investigators have reported that the calcium phosphate doping with F^- ions or Mg^{2+} ions leads to a decrease of the biodegradation rate of the material in vivo [9]. Therefore, we search for another additive to stabilize the βTCP structure.

Various ions can be incorporated into the βTCP and apatite crystal structure to replace the position of calcium or phosphorous ions but only biocompatible ones are considered here. Ca^{2+}, PO_4^{3-}, OH^-, CO_3^{2-}, and

* Corresponding author. Fax: 886-2-23940049; e-mail: double@ha.mc.ntu.edu.tw

0142-9612/98/$19.00 © 1998 Published by Elsevier Science Ltd. All rights reserved.
PII S0142-9612(98)00040-4

citrate are the main constituents for the inorganic composition of the bone. Na^+, Mg^{2+}, Cl^- and F^- are the minor elements in the hard tissue. The sodium ions are the largest amount of metallic ions stored in bone mineral after calcium and phosphorous ions. The difference of ionic radius between calcium and sodium ions is lower than 15%. Sodium ions could be expected to replace the calcium ions in the whitlokite and apatite structure at high temperatures [8]. Moreover, βTCP and apatite doped with sodium ions would have less remnant because the sodium oxide or the compounds containing Na^+ ion have lower melting and boiling point, which could be volatilized or decomposed at higher temperatures. Therefore, we try to use the precursor containing sodium ions to dope the TCP and/or apatite while preparing the high-temperature stabilized βTCP sintering body in the study.

In this experiment, we prepared a deficient HAP (d-HAP, $Ca_{10-x}(HPO_4)_x(PO_4)_{6-x}(OH)_{2-x}$, $0 < X < 2$) with nanograde particle size as the starting material. The Ca/P ratio of the prepared d-HAP is similar to that of tricalcium phosphate, about 1.5. The crystalline structure of d-HAP are the same with stoichiometric HAP (s-HAP) at room temperature [10–12], however, the d-HAP could be decomposed into βTCP and s-HAP while being heated [12–15]. According to Fowler's study on the pyrolysis reactions of octacalcium phosphate, the s-HAP could react with the pyrophosphate ions ($P_2O_7^{4-}$) and turned into βTCP around 700°C [16]. Therefore, the tetra-sodium diphosphate decahydrate (NP, $Na_4P_2O_7 \cdot 10H_2O$) containing Na^+ and $P_2O_7^{4-}$ ions was chosen as the additive while doping the d-HAP to develop high-temperature stabilized βTCP. The phase transformation or crystal structure reconstruction of d-HAP with different NP additions while being heated are also described in the study. We would also like to know the role of the pyrophosphate ions on the decomposition of d-HAP.

In the present study, we used XRD (X-ray diffraction) analysis to examine the phase transformation of the materials at different heating temperatures. The functional group of βTCP, d-HAP and d-HAP with NP addition at different temperatures were observed by FTIR (Fourier-transformed infrared) spectroscopy.

2. Materials and methods

The d-HAP with an atomic ratio Ca/P = 1.5 was prepared and is briefly described as follows. An aqueous solution of $(NH_4)_2HPO_4$ was added dropwise to a $Ca(NO_3)_2 \cdot 4H_2O$ solution at 25°C, where the pH of both the solutions were maintained at about 11 by adding the NH_4OH solution. After being mixed, the reaction solution was heated up to its boiling point and refluxed for 20 min. It was then left standing for 20 h at room temperature without stirring. The d-HAP precipitates were filtered and washed with deionized water. The products were dried at 70°C for 72 h. βTCP was prepared by heating a mixture of reagent-grade $CaHPO_4$ and $CaCO_3$ with molar ratio of 2:1 at 1000°C for 24 h. $Na_4P_2O_7 \cdot 10H_2O$ was purchased from E. Merck, 64271 Darmstadt, Germany.

The d-HAP was mixed with different quantities of $Na_4P_2O_7 \cdot 10H_2O$ in deionized water and dried at 70°C for 3 days. The well-mixed and dried cakes were ground and sieved. The samples were placed in covered platinum crucibles and heated to different temperatures at a heating rate of 3°C min^{-1} in a conventional Ni–Cr coiled furnace, and then maintained for 6 h. The samples were then quenched to room temperature.

The crystalline phases of specimens were determined by Rigaku X-ray powder diffractometer with CuK_α radiation and Ni filter. The scanning range of the samples was from 10 to 60° with a scanning speed of 4° min^{-1}. The infrared spectra were recorded using KBr pellets (1 mg sample per 300 mg KBr) on a Jasco FTIR grating instrument with slow scan and normal silt width.

3. Results

The XRD patterns of βTCP and d-HAP without the addition of $Na_4P_2O_7 \cdot 10H_2O$ at different heating temperatures are shown in Fig. 1. As seen in Fig. 1a and b, βTCP started transforming into αTCP at 1200°C. A trace of αTCP with capital 'A' topped on the peaks of Fig. 1a was found in the XRD pattern after a temperature of 1200°C. The intensity of αTCP characterized peaks increased with heating temperature. βTCP characterized peaks were still observed even after the heating temperature of 1300 °C. d-HAP were decomposed into s-HAP and βTCP at the temperature of 1150°C as shown in Fig. 1b. s-HAP peaks could be traced in the XRD patterns and their intensities were not much changed in the temperature range 1150–1300 °C. Characterized peaks of αTCP appeared at 1200 °C and increased with heating temperature as well. At 1300 °C, the inversion of βTCP to αTCP was still in progress and βTCP characterized peaks were still observed. By the way, s-HAP has the same XRD pattern as the d-HAP but is different in chemical composition. We will describe it later in Section 4.

Fig. 2 summarizes the XRD patterns of d-HAP with different quantities of NP addition in the temperature range 1150–1300°C. All the d-HAP characterized peaks disappeared and turned into s-HAP and βTCP. Fig. 2a and b represent the XRD patterns of d-HAP with 2.5 and 5 wt% NP addition, respectively. The inversion temperature of βTCP $\rightarrow$ αTCP in the d-HAP with 5 wt% NP addition was higher than that of the 2.5 wt% NP addition. As shown in Fig. 2a and b, βTCP turned into αTCP and no βTCP peaks remained once the temperature was

beyond 1250°C. The intensity of s-HAP characterized peaks gradually decreased as the quantity of NP addition increased. Comparing Fig. 2a with Fig. 1b, s-HAP characterized peaks of d-HAP with 2.5 wt% NP addition was lower than that of d-HAP without NP addition. For d-HAP with 5 wt% NP addition, only a few s-HAP peaks were still observed. Results of XRD analysis of the d-HAP with 7.5 and 10 wt% NP addition were shown in Fig. 2c and d, respectively. It showed that the more NP doped into the d-HAP, the higher phase transition temperature of βTCP to αTCP was observed. The d-HAP with 7.5 wt% NP addition could maintain the βTCP structure up to 1250°C, and d-HAP with 10 wt% NP addition could stabilize the βTCP structure beyond 1300°C. The s-HAP phase decomposed from d-HAP almost disappeared in the XRD patterns of d-HAP with 7.5 and 10 wt% NP addition. The characteristic peak of $Na_3Ca_6(PO_4)_5$ appearing at 1150°C was noteworthy. There seems some connections existing between the phase transformation temperature of βTCP to αTCP and the decomposition of $Na_3Ca_6(PO_4)_5$. At the 7.5 wt% NP addition, the $Na_3Ca_6(PO_4)_5$ peaks disappeared at a temperature between 1250 and 1300°C. The phase transformation of βTCP to αTCP occurred in the same temperature range as well. For the d-HAP with 10 wt% NP addition, the intensity of $Na_3Ca_6(PO_4)_5$ was stronger than that of d-HAP with 7.5 wt% NP addition. Though $Na_3Ca_6(PO_4)_5$ gradually disappeared with increased temperature in the d-HAP with 10 wt% NP addition, there was still some $Na_3Ca_6(PO_4)_5$ existing at the

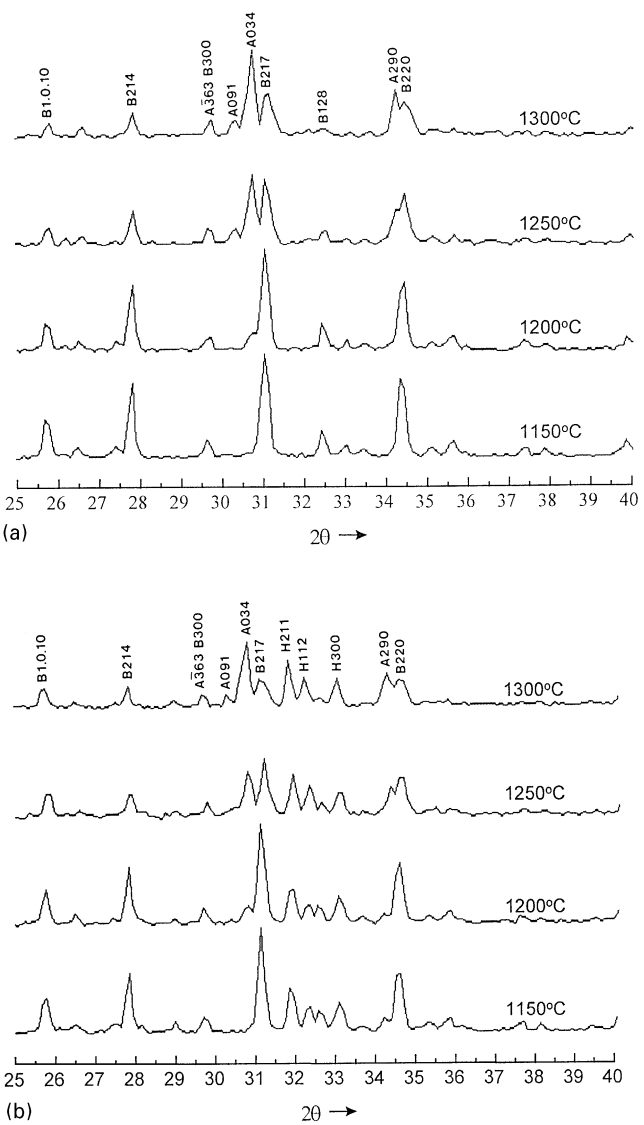

Fig. 1. X-ray diffraction patterns of βTCP and d-HAP heated at 1150, 1200, 1250 and 1300°C: (a) βTCP; (b) d-HAP (B: βTCP phase; A: αTCP phase; H: s-HAP phase).

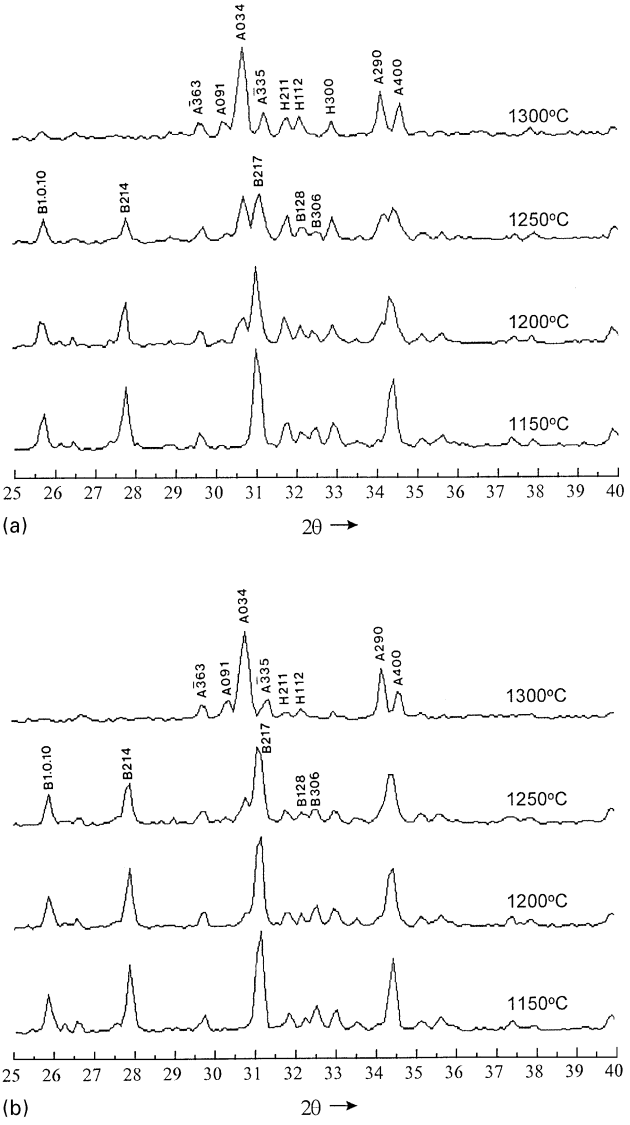

Fig. 2. X-ray diffraction patterns of d-HAP with different additions of $Na_4P_2O_7 \cdot 10H_2O$ heated at 1150, 1200, 1250 and 1300°C, respectively: (a) 2.5 wt% addition; (b) 5 wt% addition; (c) 7.5 wt% addition (characteristic peaks of $Na_3Ca_6(PO_4)_5$ phase did not appear in the patterns); (d) 10 wt% addition (B: βTCP phase; A: αTCP phase; H: s-HAP phase; ▼: $Na_3Ca_6(PO_4)_5$ phase).

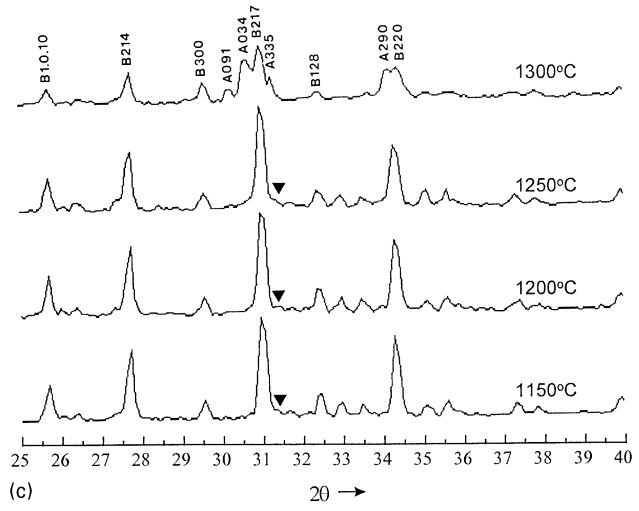

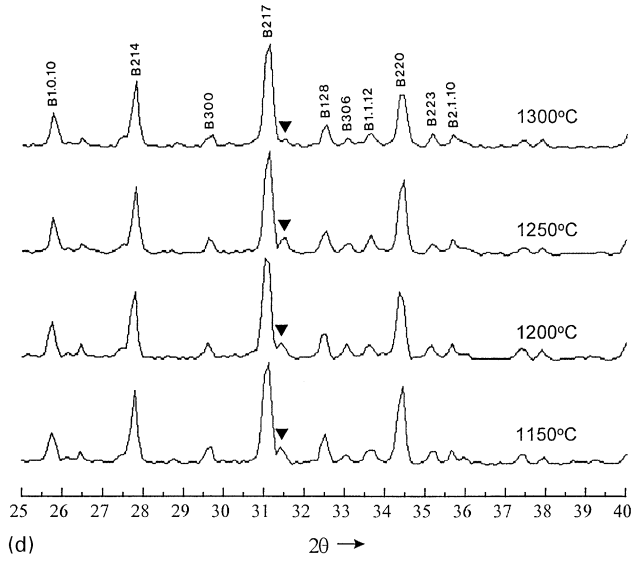

Fig. 2. (*continued*).

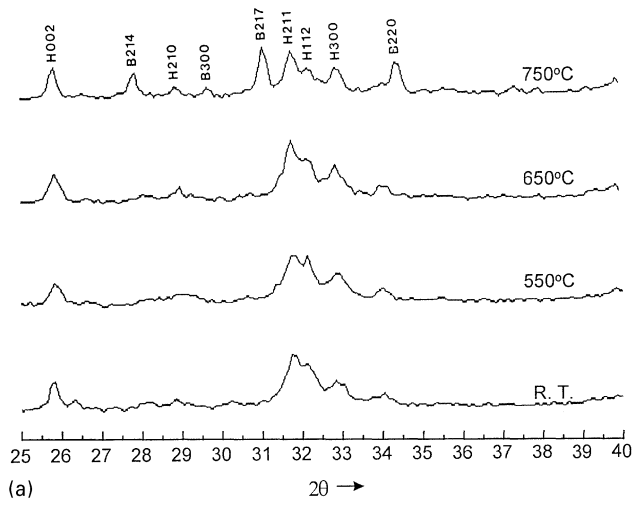

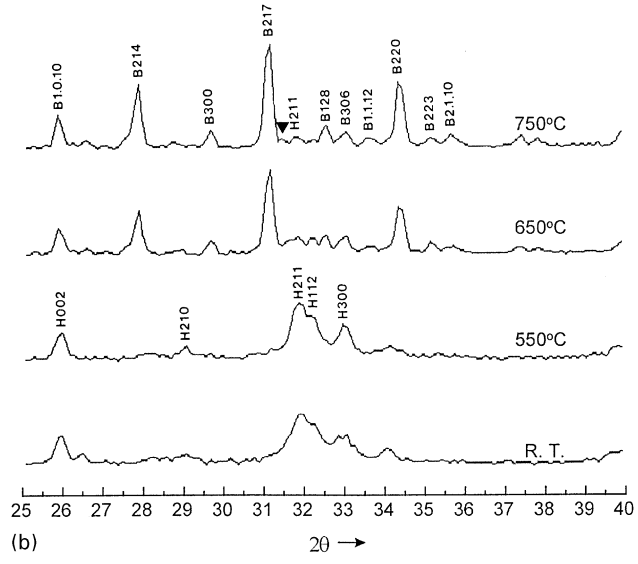

Fig. 3. X-ray diffraction patterns of d-HAP and d-HAP with 10 wt% $Na_4P_2O_7 \cdot 10H_2O$ addition at room temperature and heated at 550, 650, 750°C: (a) d-HAP; (b) 10 wt% addition (B: βTCP phase; H: s-HAP phase; ▼: $Na_3Ca_6(PO_4)_5$ phase).

temperature 1300°C. There were no αTCP characteristic peaks observed at the same temperature.

To further understand the phase transformation in the system of d-HAP with NP addition, the d-HAP and d-HAP with 10 wt % NP was prepared and heated at a relative lower temperature. Fig. 3a and b showed the XRD patterns of d-HAP and d-HAP with 10 wt% NP addition from room temperature to 750°C. There was no significant difference in XRD patterns of d-HAP below 650°C, only s-HAP observed in the pattern as shown in Fig. 3a. In Fig. 3a, βTCP peaks could be traced on the XRD patterns at the temperature of 650°C. With temperature up to 750°C, the intensity of the βTCP peaks obviously increased. On the contrary, we could observe βTCP characteristic peaks such as B217 and B220 burgeoned out on the XRD pattern of d-HAP with 10 wt% NP addition at 550°C (Fig. 3b). In addition, $Na_3Ca_6(PO_4)_5$ peaks could be observed at 750°C in Fig. 3b).

The FTIR spectrum of d-HAP heated at different temperatures were shown in Fig. 4a. The band of HPO_4^{2-} at 875 cm^{-1} decreased with the heating temperature while the band of $P_2O_7^{4-}$ at 1185 cm^{-1} slightly increased [16]. With the heating temperatures up to 750°C, the HPO_4^{2-} band almost disappeared but the $P_2O_7^{4-}$ band was formed with decreased intensity. Bands of TCP gradually appeared at 1118, 973 and 945 cm^{-1}. The spectrum of d-HAP with 10 wt% NP addition heated from room temperature to 750°C are shown in Fig. 4b. When compared to the spectrum at room temperature, the intensity of the HPO_4^{2-} band slightly decreased at 550°C. The $P_2O_7^{4-}$ band was obviously raised and the bands of TCP were found at 973 cm^{-1} at 550°C. With temperatures up to 650°C, significant TCP bands appeared at 1118, 973,

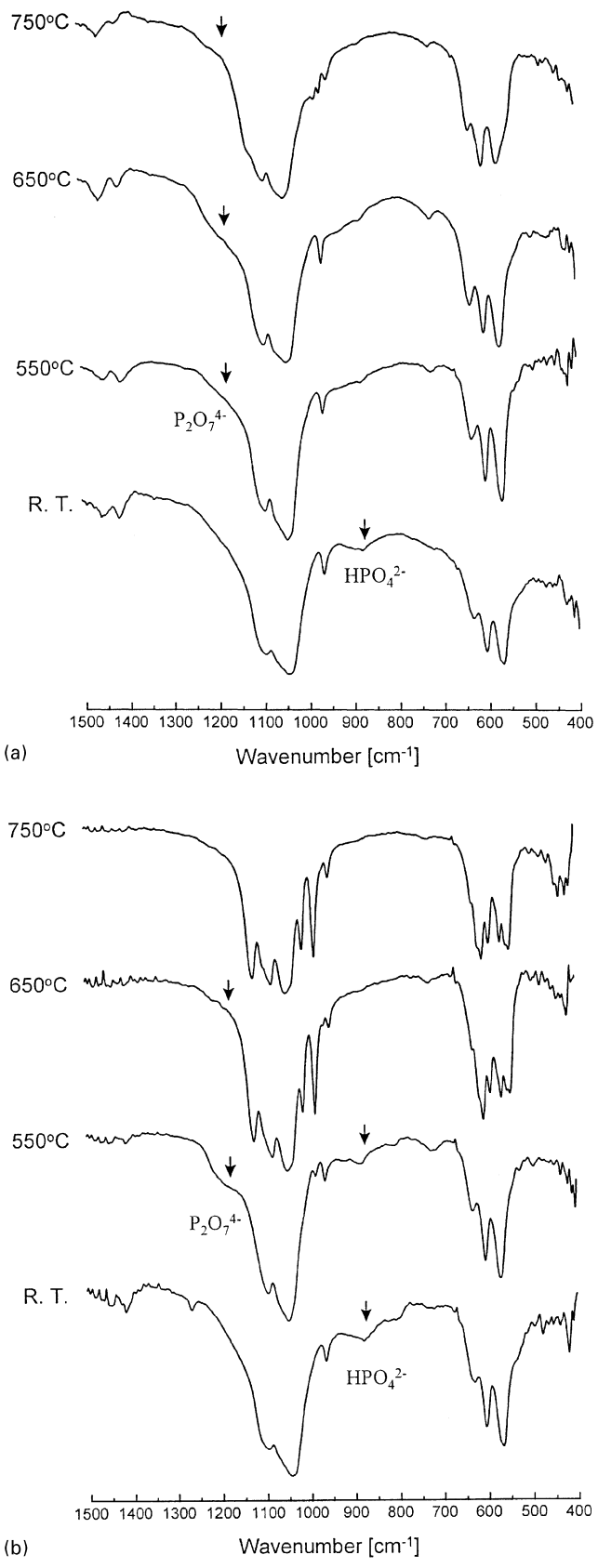

Fig. 4. FTIR spectra of d-HAP and d-HAP with 10 wt% $Na_4P_2O_7 \cdot 10H_2O$ addition at room temperature and heated at 550, 650, 750°C (a) d-HAP; (b) d-HAP with 10 wt% NP addition.

945, 603, 586, 649 and 540 cm^{-1}. Only small HPO_4^{2-} and $P_2O_7^{4-}$ bands could be traced.

4. Discussion

The Ca/P ratio of d-HAP [deficient apatite $Ca_{10-x}(HPO_4)_x(PO_4)_{6-x}(OH)_{2-x}(0 < x < 2)$] is about 1.33–1.67 with apatite crystal structure. It is known that the HPO_4^{2-} ions in d-HAP will be condensed into $P_2O_7^{4-}$ ions ($2HPO_4^{2-} \rightarrow P_2O_7^{4-} + H_2O$) when heated to about 650°C. $P_2O_7^{4-}$ ions will then react with OH^- as following formula [12]: $P_2O_7^{4-} + 2OH^- \rightarrow 2PO_4^{3-} + H_2O$. It will be accompanied with the d-HAP decomposed into βTCP and s-HAP. The total reaction can be summarized as [12, 13]

$$Ca_{10-x}(HPO_4)_x(PO_4)_{6-x}(OH)_x \rightarrow 3XCa_3(PO_4)_2 + (1-X)Ca_{10}(PO_4)_6(OH)_2 + H_2O. \quad (1)$$

Eq. (1) was supposed to have a slow reaction rate, which started at 650°C and still ongoing above 1000°C. Lee [15] suggested that the condensation of HPO_4^{2-} ions of d-HAP depend on their position in the crystal structure. The HPO_4^{2-} ions need greater energy to reach their condensation, which would lead to the condensation of HPO_4^{2-} over a wide temperature range. He thought that $P_2O_7^{4-}$ reacting with OH^- to form PO_4^{3-} is an instant reaction. The reaction will occur once $P_2O_7^{4-}$ ions are formed, therefore $P_2O_7^{4-}$ ions are difficult to observe while heating.

From the results of FTIR analysis of this study, HPO_4^{2-} band of d-HAP was hardly detected at 550°C as shown in Fig. 4a. It means that HPO_4^{2-} has been transformed into $P_2O_7^{4-}$ and did not exist at 550°C. The $P_2O_7^{4-}$ band could be traced at 550°C and appeared at 650°C with an obvious slope on the FTIR curve (Fig. 4a). We could speculate that the condensation of HPO_4^{2-} might occur before 650°C and the $P_2O_7^{4-}$ ions would be formed simultaneously. A large amount of βTCP should be formed at this temperature if $P_2O_7^{4-}$ with OH^- was an instant reaction. However, only a small amount of βTCP could be observed at this temperature as shown in Fig. 3a. We thought that the $P_2O_7^{4-}$ reacted with OH^- was not an instant reaction as described in the previous section. Fowler [16] has studied the pyrolysis reactions of octacalcium phosphate. The series reaction of octacalcium phosphate pyrolysis are as follows:

$$Ca_8H_2(PO_4)_6 \cdot 5H_2O \rightarrow 0.5Ca_{10}(PO_4)_6(OH)_2 \text{ (s-HAP)} + 1.5Ca_2P_2O_7 + 5.5H_2O, \quad (2)$$

$$0.5Ca_{10}(PO_4)_6(OH)_2 \text{ (s-HAP)} + 1.5Ca_2P_2O_7 + 5.5H_2O \rightarrow 2Ca_3(PO_4)_2 + Ca_2P_2O_7 + 6H_2O. \quad (3)$$

It showed that the pyrolysis of $CaHPO_4$ in the range of 325–450°C yielded $Ca_2P_2O_7$ (Eq. (2)) and βTCP would

be obtained from the $Ca_2P_2O_7$ and s-HAP reaction around 700°C. The study revealed that the $P_2O_7^{4-}$ ions reaction with OH^- did not occur immediately. We speculated that the $P_2O_7^{4-}$ ions should be accumulated to a critical concentration to react with OH^- and then induce d-HAP decomposition. The concentration of $P_2O_7^{4-}$ might play an important role on the decomposition of d-HAP. Since $P_2O_7^{4-}$ could be traced even at temperatures up to 750°C, it seemed that the $P_2O_7^{4-}$ reacting with OH^- to form PO_4^{3-} should occur over a wide temperature range. The rate of d-HAP conversion into βTCP and s-HAP should depend on the rate of $P_2O_7^{4-}$ and OH^- reaction instead of HPO_4^{2-} condensation.

The HPO_4^{2-} band of d-HAP with 10 wt% NP showed no significant difference from room temperature to 550°C (Fig. 4b). Comparing Fig. 4b with Fig. 4a, the $P_2O_7^{4-}$ band of d-HAP with 10 wt% NP addition was more obvious than that of d-HAP without NP addition from room temperature to 550°C. Most of the $P_2O_7^{4-}$ ions bands appearing in d-HAP with 10 wt% NP addition at 550°C (Fig. 4b) was coming from the $Na_4P_2O_7 \cdot 10H_2O$ addition. The foreign $P_2O_7^{4-}$ ions coming from NP addition would raise the concentration of $P_2O_7^{4-}$ ions in the system and lead to the d-HAP decomposition at a lower temperature around 550°C (Fig. 1b). According to Eq. (1), d-HAP should be converted into βTCP and s-HAP at 650°C. However, s-HAP peaks almost disappeared and βTCP progressively produced peaks in the XRD pattern of d-HAP with 10 wt% NP addition at the temperature of 650°C (Fig. 3b). The reaction might occur in the system as follows:

$$3Ca_{10}(PO_4)_6(OH)_2 + 2Na_4P_2O_7 \rightarrow 10Ca_3(PO_4)_2 + 3Na_2O + 2NaPO_3 + 3H_2O. \quad (4)$$

It reflects that the NP doped into d-HAP not only induced the d-HAP decomposition at a lower temperature but also reacted with s-HAP to produce more βTCP in the system.

It is known that the transformation of βTCP to αTCP started at 1180°C. From XRD analysis, βTCP still existed while βTCP or d-HAP without NP addition was heated up to 1300°C (Fig. 1a and b). The results reveal that the transformation rate of βTCP to αTCP takes place at a slow pace. We observe that the intensity of βTCP characteristic peaks in Fig. 2a and b are higher than that of d-HAP at 1250°C (Fig. 1a). The authors speculated that NP might stabilize βTCP at higher temperatures or might increase the conversion temperature of βTCP to αTCP, once it was doped into d-HAP.

In Fig. 2c and d, $Na_3Ca_6(PO_4)_5$ could be observed in the XRD patterns of the d-HAP with 7.5 and 10 wt% NP addition. The $Na_3Ca_6(PO_4)_5$ with chemical composition of $2.4CaO \cdot 0.6Na_2O \cdot P_2O_5$ was found by Ando [19] in the study of the binary phase diagram of $Ca_3(PO_4)_2$–$NaCaPO_4$(rhenanite). The phase could be easily formed in the range of $2.6CaO \cdot 0.4Na_2O \cdot P_2O_5$ to $2.4CaO \cdot 0.6Na_2O \cdot P_2O_5$ [19,20]. Lin [21], studied the sintering behavior of βTCP bioceramics with NP addition and observed $Na_3Ca_6(PO_4)_5$ in XRD patterns with βTCP doped with NP up to 5 wt%. The intensity of $Na_3Ca_6(PO_4)_5$ characteristic peaks increased with the quantity of NP added to the system. Suchanek [22] doped $Na_4P_2O_7$ into hydroxyapatite to promote the sintering process, where $Na_3Ca_6(PO_4)_5$ could be observed in the system.

Schaeken [8] heated mixtures of $CaHPO_4$, $CaCO_3$ and Na_2CO_3 at temperatures between 700°C and 1000°C and found that sodium was incorporated in the crystal structure of whitlockite and apatite. It is known that the mixture of $CaHPO_4$ and $CaCO_3$ could produce βTCP [10], and the Na_2CO_3 would be decomposed into Na_2O and CO_2 in the same temperature range 700–1000°C. According to the results of Schaeken, Na_2O could be assumed to react with βTCP and form the sodium-containing whitlockite in the temperature range 700–1000°C. In the present study, sodium-containing whitlockite is quite possible to be formed in the system of d-HAP with NP addition as expressed in eq. (4). In the system, βTCP would react with Na_2O and then form sodium-containing whitlockite once d-HAP decomposed. $Na_3Ca_6(PO_4)_5$ was formed around 750°C (Fig. 3b), that might be the reaction product of the βTCP and Na_2O. Comparing Fig. 2c with d, we observed that the intensity of $Na_3Ca_6(PO_4)_5$ characteristic peaks increased with the quantity of NP in the system. The intensity had a negative tendency with temperature and would finally disappear around the temperature of 1250–1300°C.

From the phase diagram of $Mg_3(PO_4)_2$–$Ca_3(PO_4)_2$ system, Mg^{2+} ions incorporating into the TCP structure are effective in stabilizing the βTCP structure and raising the βTCP $\rightleftharpoons$ αTCP transforming temperature from 1180 up to 1500°C [18, 19]. Kreidler and Hummel [23] investigated the system of $Ca_3(PO_4)_2$–$Zn_3(PO_4)_2$ and found that the Zn^{2+} ion incorporating into βTCP structure has the same effect as that of Mg^{2+} ions in the βTCP crystal structure. Ando [24] also found that magnesia, alumina and ferric oxides could effectively stabilize the βTCP phase and prevent the inversion of βTCP $\rightarrow$ αTCP while heating. However, the effect of Na^+ ions incorporating into the TCP structure depended on its concentration in the structure because Na_2O was easily sublimble. In this study, the transformation temperature of βTCP $\rightarrow$ αTCP increased with the NP addition as shown in Fig. 2a–d. It proved that the Na^+ ion incorporating into the TCP crystal structure could effectively stabilize the βTCP structure and keep βTCP $\rightarrow$ αTCP from transformation. Though Na^+ ions would stabilize the βTCP structure only up to 1300°C, the temperature is enough to obtain high densified βTCP ceramic after sintering.

5. Conclusion

The decomposition of d-HAP as Eq. (1) was supposed to have a slow reaction which started at 650°C and still ongoing above 1000°C. It is known that the HPO_4^{2-} ions in d-HAP will condense into $P_2O_7^{4-}$ ions ($2HPO_4^{2-} \rightarrow P_2O_7^{4-} + H_2O$) when heated to about 650°C. $P_2O_7^{4-}$ ions will then react with OH^- as $P_2O_7^{4-} + 2OH^- \rightarrow 2PO_4^{3-} + H_2O$. From the study, we could speculate that the condensation of HPO_4^{2-} might occur before 650°C and the $P_2O_7^{4-}$ ions would be formed simultaneously. Since $P_2O_7^{4-}$ could be traced even at temperatures up to 750°C, it seemed that the $P_2O_7^{4-}$ reacting with OH^- forming PO_4^{3-} should occur over a wide temperature range. The rate of d-HAP conversion into βTCP and s-HAP should depend on the rate of the $P_2O_7^{4-}$ and OH^- reaction instead of the HPO_4^{2-} condensation.

NP doped into d-HAP not only induced the d-HAP decomposition at lower temperature but also stabilized the βTCP crystal structure at higher temperatures or increased the conversion temperature of βTCP to αTCP. In this study, the transformation temperature of βTCP $\rightarrow \alpha$TCP increased with the NP addition. It proved that the Na^+ ions incorporating into the TCP crystal structure could effectively stabilize the βTCP structure and keep βTCP $\rightarrow \alpha$TCP from transformation. By mixing NP with d-HAP, we could obtain a pure βTCP sintering body at the temperature up to 1300°C without αTCP transformation.

References

[1] Klein CPAT. Interaction of biodegradable β-whitlockite ceramics with bone tissue: an in vivo study. J Biomed Mater Res 1984;18:845–59.

[2] Kotani S, Fujita Y, Kitsugi T, Nakamura T, Yamamuro T, Ohtsuki C, Kokubo T. Bone bonding mechanism of β-tricalcium phosphate. J Biomed Mater Res 1991;25:1303–15.

[3] Jarcho M. Calcium phosphate ceramics as hard tissue prosthetics. Clin Orthop Rel Res 1981;157:259–78.

[4] Katthagen BD. Bone regeneration with bone substitutes. Berlin, Heidelberg: Springer, 1987.

[5] Dickens B, Schroeder LW, Brown WE. Crystallographic studies of the role of Mg as a stabilizing impurity in β-$Ca_3(PO_4)_2$. I. The crystal structure of pure β-$Ca_3(PO_4)_2$. J Sol State Chem 1974; 10:232–48.

[6] Schroeder LW, Dickens D, Brown WE. Crystallographic studies of the role of Mg as a stabilizing impurity in β-$Ca_3(PO_4)_2$. II. Refinement of Mg-containing β-$Ca_3(PO_4)_2$. J Sol State Chem 1977;22:253–62.

[7] Bigi A, Foresti E, Gregorini R, Ripamonti A, Roveri N, Shah JS. The role of magnesium on the structure of biological apatites. Calcif Tissue Int 1992;50:439–44.

[8] de Groot K. Bioceramics of calcium phosphate. Boca Raton, FL: CRC Press, 1983.

[9] Klein CPAT, Driession AA, de Groot K. Biodegradation of calciumphosphate ceramics-ultrastructural geometry and dissolubility of different calcium phosphate ceramics. In Grote JJ, editors. Biomaterials in Otology: The Hague: Nijhoff, Martinus, 1984.

[10] Aoki H. Medical application of hydroxyapatite. Ishiyaku Euro America, Inc. Tokyo, St. Louis Takayama Press, 1994.

[11] Asada M, Miura Y, Osaka A, Oukami K, Nakamura S. Hydroxyapatite crystal growth on calcium hydroxyapatite ceramics: J Mater Sci 1988;23:3202–5.

[12] Mortier A, Lemaitre J, Rodrique L, Rouxhet PG, Synthesis and thermal behavior of well-crystallized calcium-deficient phosphate apatite. J Solid State Chem 1989;78:215–19.

[13] Ishikawa K, Ducheyne P, Radin S. Determination of the Ca/P ratio in calcium-deficient hydroxyapatite using X-ray diffraction analysis. J Mater Sci Mater Med 1993;4:165–8.

[14] Yubao L, Klein CPAT, de Wijn J, van De Meer S. Preparation and characterization of nanograde osteoapatite-like rod crystals. J Mater Sci Mater Med 1994;5:252–5.

[15] Yubao L, Klein CPAT, de Wijn J, van De Meer S. Morphology and composition of nanograde calcium phosphate need-like crystals formed by simple hydrothermal treatment. J Mater Sci Mater Med 1994;5:326–331.

[16] Fowler BO, Moreno EC, Brown WE. Infra-red spectra of hydroxyapatite, octacalcium phosphate and pyrolysed octacalcium phosphate. Arch Oral Biol 1996;11:477–92.

[17] Reser MK. Phase diagrams for ceramists. Ceramic Drive, 65 Ohio Columbus: The American Ceramic Society, 1964.

[18] Mathew M, Schroeder LW, Dickens B, Brown WE. The crystal structure of α-$Ca_3(PO_4)_2$. Acta Crystallogr B33:1325–33.

[19] Ando J. Phase diagrams of $Ca_3(PO_4)_2$–$Mg_3(PO_4)_2$ and $Ca_3(PO_4)_2$–$CaNaPO_4$ systems. Bull Chem Soc Jpn 1958;31: 201–5.

[20] Ando J, Matsuno S $Ca_3(PO_4)_2$–$CaNaPO_4$ system. Bull Chem Soc Jpn 1968;41:342–7.

[21] Lin FH, Hon MH. Sintering β-tricalciumphosphate bioceramics with $Na_4P_2O_7 \cdot 10H_2O$. J Mater Sci Lett 1987;6:501–3.

[22] Suchanek W, Yashima M, Kakihana M, Yoshimura M. Hydroxyapatite ceramics with selected sintering additives. Biomaterials 1997;18:923–33.

[23] Kreidler ER, Hummel FA. Phase relationships in the system SrO–P_2O_5 and the influence of water vapor on the formation of $Sr_4P_2O_9$. Inorg Chem 1967;884–91.

[24] Ando J. Tricalcium phosphate and its variation. Bull Chem Soc Jpn 1958;31:196–201.